

## Mixed Orientation State Induced by Expansion Flow of a Thermotropic Liquid-Crystalline Polymer

David K. Cinader, Jr., and Wesley R. Burghardt\*

Department of Chemical Engineering, Northwestern University, Evanston, Illinois 60208

Received July 20, 1998

Revised Manuscript Received October 20, 1998

**Introduction.** Technological applications of thermotropic liquid-crystalline polymers (TLCPs) rely on exceptional physical properties that, in turn, reflect the degree of molecular orientation induced by processing flows. While lyotropic liquid-crystalline polymers must be processed in solution, TLCPs may be melt-processed by extrusion and injection molding. These operations involve complex kinematics with mixed shear and extension, so that it is difficult to predict the final orientation state. Previously, orientation has been studied in molded samples.<sup>1–3</sup> However, this does not allow isolation of the effects of complex flow history from those due to the transient, nonisothermal nature of injection molding. For this reason, we have constructed an apparatus to allow in situ measurement of molecular orientation of TLCPs in channel flows, like those encountered during processing. This communication describes our experimental setup and documents how expansion flows strongly influence molecular orientation and lead to complex, mixed orientation states.

Even in shear flow, development of macroscopic orientation in LCPs involves complex phenomena.<sup>4</sup> Orientation is typically disrupted by defects, leading to “domains” of size on the order of microns. In lyotropic LCPs at low shear rates, it is understood that hydrodynamic torque promotes time-dependent director rotation, known as *tumbling*,<sup>5</sup> leading to a proliferation of defects and disruption of molecular orientation.<sup>4,6</sup> Understanding of TLCPs is less advanced; for instance, it has not been conclusively shown whether commercial TLCP copolyesters exhibit tumbling or alignment in shear.

Channel flows incorporating contractions or expansions introduce additional complexity in that (i) extensional gradients are present and (ii) the relative strength of shear and extension will vary as a function of position within the flow. In studying a lyotropic LCP, Bedford and Burghardt<sup>7</sup> argued that extensional gradients in a slit-contraction flow induce a transition from tumbling to flow-aligning behavior near the midplane of the flow field, leading to a strong enhancement in orientation measurements averaged through the sample thickness. Such orientation enhancement may also reflect the drawing of tumbling orbits toward the shear plane in regions of the flow where extension, while still present, is insufficient to induce a transition to flow alignment.<sup>8</sup>

In slit-expansion flows, fluid deceleration is accompanied by stretching *transverse* to the flow direction (i.e., into the vorticity direction of the base-shearing flow).<sup>8</sup> In general terms, slit expansions are thus expected to

lead to decreases in average orientation. This has been observed in recent studies of a model lyotropic LCP.<sup>8</sup> As before, extension will dominate the dynamics at the midplane of slit-expansion flows, while shear will dominate near the walls. The basic consequences of such mixed kinematics have been examined using stability analysis and simulation of the director evolution equations contained in Ericksen’s transversely isotropic fluid (TIF) model.<sup>8</sup> For tumbling LCPs, extension superimposed on shear will induce drift of tumbling orbits toward the vorticity direction, with increasing rate as the midplane is approached. The qualitative response predicted in flow-aligning materials is different. Near the walls, the stable flow-aligned orientation state resists the effects of extension; however, as the midplane is approached, there is an abrupt transition where vorticity alignment is stabilized by the transverse stretching within the central portion of the flow. This suggests that two discrete orientation states should develop as a function of depth in the expansion region of a slit-expansion flow.

Radial outflow between disks involves a very similar mixture of inhomogeneous shear and extension out of the shear plane. Rey has performed Leslie–Ericksen simulations for this geometry for flow-aligning nematics and demonstrated such a transition to an out-of-plane mode as a function of depth, modulated by orientational boundary layers.<sup>9,10</sup> It is difficult to anticipate the applicability of these simulations, performed at a modest Ericksen number on a monodomain orientation state, to conditions encountered in experiments on polymeric LCPs, where high viscosities lead to very large Ericksen numbers, and samples typically exhibit a “polydomain” texture.

**Experimental Section.** We have studied a commercial resin, Xydar SRT900, provided by Amoco. This is an aromatic copolyester of unknown exact composition, supplied without fillers. We have processed it at 340 °C as suggested by the manufacturer. Frayer and Huspeni<sup>11</sup> report thermal and rheological data on similar resins with higher melting points. Rheology is a strong function of shear and thermal history in thermotropic random copolyesters, due to the effect of prior deformation on the orientation and texture of the LCPs, and the possibilities of melt-phase chemistry (transesterification and/or additional polymerization) and melt recrystallization. Frayer and Huspeni advocate material testing under conditions as close as possible to processing.<sup>11</sup> In this study, our use of an extruder to provide a steady flow was motivated by the fact that this allows for a constant (albeit complex) thermal and flow history, irrespective of an experiment’s duration. The polymer was dried in a vacuum oven prior to use. A slight scent of acetic acid in the extrudate indicates that a small amount of additional polymerization occurs in the melt phase; however, there was no gross extrudate distortion due to bubbles or flow instabilities.

X-ray scattering is used to measure orientation in channel flows. Figure 1 depicts the extrusion die designed and constructed for these studies. Flow geometries are defined by interchangeable 1 mm thick steel spacers sandwiched between two temperature-controlled steel blocks. These blocks feature V-shaped trenches that allow incident and scattered radiation to

\* Corresponding author. Phone: 847-467-1401. Fax: 847-491-3728. E-mail: w-burghardt@nwu.edu.

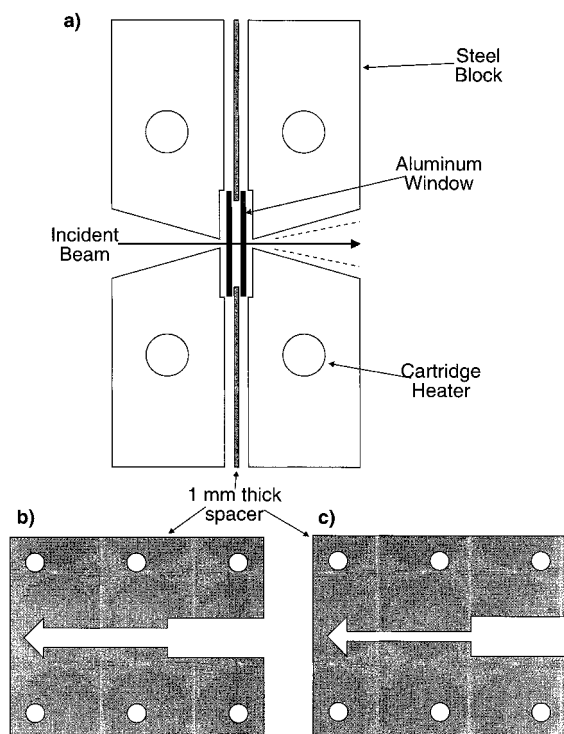


**Figure 1.** Schematic of the extrusion die. (a) Exploded cross section shows positioning of windows and spacer. Flow direction is perpendicular to the plane of the page. (b) Spacer for 1:2 slit-expansion flow. (c) Spacer for 1:4 slit-expansion flow. Polymer is delivered from one steel block through a manifold region and then flows through the slit from left to right.

enter and exit the flow cell. At the bottom of the trenches, 1 mm thick aluminum windows contain the polymer. The aluminum windows diffract at wider angles than the scattering from the polymer; this diffracted radiation is blocked by a lead mask, while a beam stop blocks the transmitted beam. The flow channel defined by the spacer is 1 mm thick, 110 mm long, and up to 20 mm wide. The incident beam spot size was approximately 0.7 mm square. Here, we present results for 1:2 and 1:4 slit expansion flows, in which the upstream channel width is 10 and 5 mm,

respectively. The polymer is melted and pumped using a single screw extruder manufactured by Randcastle, Inc. (Microtruder RCP-0500) which provides flow rates of 1–10 g/min using a screw diameter of 1/2". For this set of experiments we have used flow rates of 5.4 g/min for the 1:2 expansion and 4.8 g/min for the 1:4 expansion; other experiments showed that orientation depends only weakly on flow rate.

X-ray scattering experiments were performed on beamline 5-BM at the Advanced Photon Source of Argonne National Laboratory. Bending magnet radiation with an energy of 25 keV was chosen to reduce absorption from the aluminum windows and to confine the polymer scattering to small angles, allowing collection through the trenches in the die. Two-dimensional scattering patterns were collected using a wire detector. At a resolution of  $256 \times 256$  pixels, scattering patterns were collected with exposures of 30 s.

**Results and Discussion.** Figure 2 shows a perspective view of the 1:4 sharp expansion and representative scattering patterns measured along the centerline. Upstream of the expansion, the two scattering peaks perpendicular to the flow direction are a typical manifestation of average orientation of the nematic phase in the downstream direction. The peak as a function of scattering angle is attributed to correlation in the lateral packing between rodlike molecules in the nematic phase. Scattering from rodlike objects occurs predominantly at right angles to the rod axis; thus, molecular orientation along the downstream direction leads to a scattering peak transverse to the flow direction, and vice versa.

In the expansion region, the scattering patterns show a loss in the intensity of the peaks associated with downstream orientation, and the simultaneous growth of nematic peaks indicating development of transverse orientation. In part of the expansion region, the transverse orientation even becomes stronger than the flow orientation! The definition of the two sets of peaks is indicative of two discrete orientation populations. Recognizing that the relative importance of shear and extension varies as a function of depth, we surmise that extension dominates near the midplane, pulling the orientation into the transverse direction, while shear

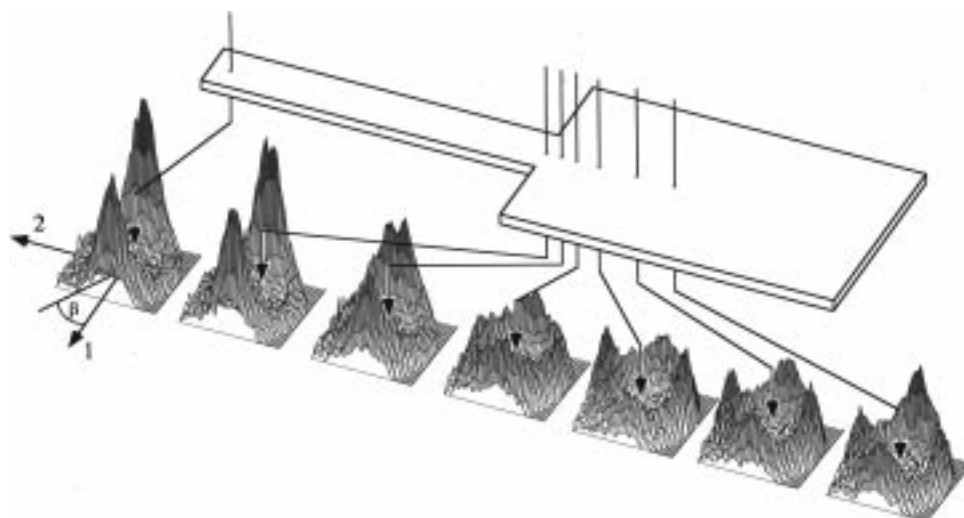


**Figure 2.** Perspective view of the 1:4 expansion flow field, showing surface plots of two-dimensional scattering patterns. The scattering peak occurs as a wave vector  $q^* = 1.14 \text{ \AA}^{-1}$ , corresponding to a lateral packing distance  $d \sim 2\pi/q^* = 5.51 \text{ \AA}$ . Patterns were collected at axial positions of  $-42, 0, 2, 4, 7, 12$ , and  $18 \text{ mm}$  downstream of the expansion. Flow direction is from left to right. Axes on the first pattern define the coordinates used to quantify anisotropy in the scattering.

dominates near the walls (i.e., the aluminum windows), maintaining orientation in the downstream direction. This evidence of two coexisting orientation states is consistent with expectations of how a flow-aligning material would behave in this type of flow; however, enhancements observed in slit-contraction flows for this material suggest that it may be of the tumbling type.<sup>12</sup>

After the expansion region the transverse peaks gradually disappear while the downstream peaks intensify, indicating a diminishing fraction of the fluid oriented transverse to the flow direction. Past the expansion, the transverse extensional gradients disappear, and accumulation of shear strain to re-establish a downstream orientation in the subsequent slit flow. This type of evolution in average orientation in channel flows has been proposed by Wissbrun<sup>13</sup> as a possible explanation for anomalies in capillary rheometry of thermotropic LCPs; however, in Wissbrun's picture shear acts to reduce orientation induced by a sharp contraction, whereas here shear acts to re-establish orientation that has been disrupted by an expansion.

X-ray scattering measurements in LCPs are often expressed in terms of an orientation parameter to characterize the degree of molecular orientation. In previous work,<sup>14</sup> we adopted the analysis procedures of Mitchell and Windle,<sup>15</sup> which assumes a uniaxial distribution of orientation. While appropriate for flows which promote uniaxial orientation (e.g., fiber spinning), such an analysis is already questionable in shear flows, which have been demonstrated to generate biaxial distributions of orientation in LCPs.<sup>16</sup> In channel flows such as those considered here, the complexities of the orientation states apparent in Figure 2 undermine interpretation of the results using a standard order parameter analysis. Instead, we adopt a simpler characterization of anisotropy in the scattering pattern, computed from an azimuthal scan of the intensity taken at a scattering angle corresponding to peak intensity. The scan is normalized and background scattering is subtracted using procedures described elsewhere.<sup>8,14</sup>

A point on the azimuthal scan may be represented by a unit vector,  $\mathbf{u}$ , such that  $u_1 = \cos \beta$  and  $u_2 = \sin \beta$  ( $\beta$  is the azimuthal angle). A weighted average of the second moment tensor of  $\mathbf{u}$  provides a simple representation of anisotropy in the scattering pattern:

$$\langle \mathbf{u}\mathbf{u} \rangle = \begin{bmatrix} \langle u_1 u_1 \rangle & \langle u_1 u_2 \rangle \\ \langle u_1 u_2 \rangle & \langle u_2 u_2 \rangle \end{bmatrix} = \begin{bmatrix} \langle \cos^2 \beta \rangle & \langle \sin \beta \cos \beta \rangle \\ \langle \sin \beta \cos \beta \rangle & \langle \sin^2 \beta \rangle \end{bmatrix} \quad (1)$$

In this expression,  $\langle \dots \rangle$  represents an average weighted by the azimuthal intensity distribution  $I(\beta)$ . For example, the average is given as

$$\langle \cos^2 \beta \rangle = \frac{\int_0^{2\pi} \cos^2 \beta I(\beta) d\beta}{\int_0^{2\pi} I(\beta) d\beta} \quad (2)$$

For centerline measurements, symmetry dictates that the off-diagonal terms in eq 1 should be zero. Under these conditions, anisotropy may be characterized by taking the difference  $\langle u_1 u_1 \rangle - \langle u_2 u_2 \rangle = \langle \cos^2 \beta \rangle - \langle \sin^2 \beta \rangle$ , which we refer to as an *anisotropy factor*. Recognizing that scattering from rodlike molecules is concentrated

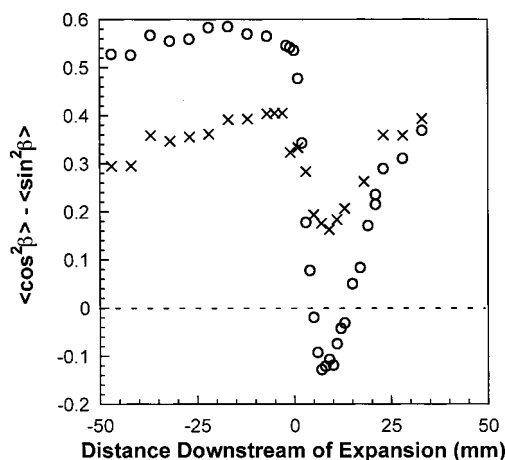


**Figure 3.** Anisotropy factor measured along the centerline in 1:4 (○) and 1:2 (×) sharp expansions as a function of the distance downstream of the expansion.

normal to the molecular axis, we adopt a coordinate system in which the 1-axis is oriented *transverse* to the flow direction (see Figure 2). This leads to the expedient result that the anisotropy factor approaches values of +1 for perfect orientation in the flow direction and -1 for perfect orientation transverse to the flow direction. As in all bulk measurements of molecular orientation,<sup>4</sup> the anisotropy factor reflects both the local distribution of molecular orientation around the director and the distribution of director orientations in the sample. In these slit-contraction flows, the degree of orientation is also averaged through the full sample thickness,<sup>8</sup> where the X-ray beam encounters varying shear and extension rates, and presumably, orientation states.

Figure 3 plots the anisotropy factor as a function of distance downstream for the 1:2 and 1:4 expansion flows. While both show significant orientation upstream of the expansion, anisotropy in the 1:4 flow exceeds that in the 1:2 flow. This probably reflects the combined effects of higher shear rates in the narrower upstream channel and stronger extension in the entry region for the 1:4 geometry. In both flows, a sudden loss of orientation is observed in the expansion region. The loss of orientation is greater for the more severe 1:4 expansion, where the transverse extension rates and total extensional strain will both be greater than those in the 1:2 flow. The anisotropy factor temporarily drops below zero in the 1:4 flow, again reflecting the fact that the orientation induced by the transverse extension exceeds the downstream alignment promoted by the base shearing flow. Downstream of the expansion, the anisotropy factor recovers as shear once again dominates the flow field and induces orientation in the downstream direction. Far downstream of the expansions, the orientation approaches nearly the same value for both geometries. This is expected since both flow channels have the same width in this region.

To summarize, we have demonstrated *in situ*, quantitative measurements of orientation in channel flows of a commercial thermotropic liquid-crystalline polymer. In slit-expansion flows, transverse extension in the expansion region has a profound effect on the average molecular orientation state. In particular, X-ray scattering reveals a coexistence of two populations of orientation, in the downstream and transverse directions. This is believed to reflect spatial variation in the orientation state within the slit-expansion flow, where



extension in the midplane region leads to transverse alignment, while shear at the walls continues to promote downstream orientation. In a 1:4 expansion flow, transverse extension is sufficiently strong to induce a flip in the average orientation direction.

**Acknowledgment.** We thank Victor Ugaz and Franklin Caputo for help with the X-ray scattering experiments. This work was funded by an AFOSR MURI and performed at the DuPont–Northwestern–Dow Collaborative Access Team (DND-CAT) Synchrotron Research Center located at Sector 5 of the Advanced Photon Source. DND-CAT is supported by the E.I. DuPont de Nemours & Co., the Dow Chemical Company, the National Science Foundation through Grant DMR-9304725, and the State of Illinois through the Department of Commerce and the Board of Higher Education Grant IBHE HECA NWU 96. Use of the Advanced Photon Source was supported by the U.S. Department of Energy, Basic Energy Sciences, Office of Energy Research under Contract No. W-31-102-Eng-38. We also thank Barry Dean of Amoco for supplying the Xydar SRT900 resin.

## References and Notes

- (1) Heynderickx, I.; Paridaans, F. *Polymer* **1993**, *34*, 4068.
- (2) Jansen, J. A. J.; Paridaans, F. N.; Heynderickx, I. E. J. *Polymer* **1994**, *35*, 2970.
- (3) Pirnia, A.; Sung, C. S. P. *Macromolecules* **1988**, *21*, 2699.
- (4) Burghardt, W. R. *Macromol. Chem. Phys.* **1998**, *199*, 471.
- (5) Burghardt, W. R.; Fuller, G. G. *J. Rheol.* **1990**, *34*, 959.
- (6) Hongladarom, K.; Burghardt, W. R.; Baek, S. G.; Cementwala, S.; Magda, J. J. *Macromolecules* **1993**, *26*, 772.
- (7) Bedford, B. D.; Burghardt, W. R. *J. Rheol.* **1996**, *40*, 235.
- (8) Cinader, D. K., Jr.; Burghardt, W. R. *Polymer*, in press.
- (9) Rey, A. D. *J. Rheol.* **1990**, *34*, 919.
- (10) Rey, A. D. *J. Non-Newtonian Fluid Mech.* **1991**, *40*, 177.
- (11) Frayer, P. D.; Huspeni, P. J. *J. Rheol.* **1990**, *34*, 1199.
- (12) Cinader, D. K., Jr.; Burghardt, W. R. To be published.
- (13) Wissbrun, K. F. *J. Rheol.* **1993**, *37*, 777.
- (14) Hongladarom, K.; Ugaz, V. M.; Cinader, D. K.; Burghardt, W. R.; Quintana, J. P.; Hsiao, B. S.; Dadmun, M. D.; Hamilton, W. A.; Butler, P. D. *Macromolecules* **1996**, *29*, 5346.
- (15) Mitchell, G. R.; Windle, A. H. In *Developments in Crystalline Polymers-2*; Basset, D. C., Ed.; Elsevier Applied Science Publishers Ltd.: London, 1988; p 115.
- (16) Hongladarom, K.; Burghardt, W. R. *Macromolecules* **1994**, *27*, 483.

MA981139L